

# Synthesis and characterization of high-energy ball milled nanostructured Fe<sub>50</sub>Ni<sub>50</sub>

A. Djekoun<sup>a,\*</sup>, A. Otmani<sup>a</sup>, B. Bouzabata<sup>a</sup>, L. Bechiri<sup>a</sup>,  
N. Randrianantoandro<sup>b</sup>, J.M. Greneche<sup>b</sup>

<sup>a</sup> *Laboratoire de Magnétisme et de Spectroscopie des Solides, Faculté des Sciences,  
Université Badji Mokhtar, B.P. 12, 23000 Annaba, Algeria*

<sup>b</sup> *Laboratoire de Physique de l'Etat Condensé, UMR CNRS 6087, Université du Maine,  
72085 Le Mans Cedex 9, France*

Available online 19 January 2006

## Abstract

Mechanical alloying is a non-equilibrium process for materials synthesis. It has been used to obtain nanocrystalline binary system FeNi.

Fe and Ni elemental powders have been ball milled in a planetary mill (Pulverisette 7, Fritsch) for various times up to several hours. The morphology of the powders was examined using scanning electron microscopy (SEM). X-ray diffraction (XRD) has been employed to follow the structural evolution during the ball milling process. The X-ray patterns were analysed by the MAUD procedure, which is based on the Rietveld method combined with a Fourier analysis, well adapted for broadened diffraction peaks. The grain size was found to be about 5 nm and the residual strain was about 0.021% after 322 h of milling. The as-milled samples, characterized by Mössbauer spectroscopy (MS) contain a mixture of  $\alpha$  (bcc) and  $\gamma$  (fcc) phases after 48 h of ball milling.

© 2005 Elsevier B.V. All rights reserved.

**Keywords:** Nanostructure; Mechanical alloying; Mössbauer spectroscopy; FeNi

## 1. Introduction

Due to their potential applications in various areas (new alloys and ceramics, catalysts, high diffusivity materials, ...) there is a great interest in developing nanocrystalline materials [1–4]. These are polycrystalline powders with grain sizes of few nanometers and a large interface fraction compared to that of the crystal exhibit non-conventional physical, chemical and mechanical properties [5]. Mechanical alloying process allows to prepare nanocrystalline alloys or nanostructured powders that cannot be obtained by conventional methods of synthesis. The scenario consists in successive fragmentation and welding stages, in conjunction with atomic diffusion between adjacent layers. The deformation of the microcrystalline phase originates from dislocations during the early stage of milling, then the increasing deformation gives rise to fractures into submicrometric grains. This mechanism leads to a material

composed of ultrafine crystalline grains, about 10 nm large, separated by non-coherent interfaces or grain boundaries. Consequently, mechanical alloying, which is a dry and high-energy milling process, has attracted considerable interest in recent years. Indeed, this process was applied to a wide range of materials, leading to metastable and unstable phases under highly non-equilibrium conditions: amorphous, quasi-crystalline and nanocrystalline phases, extended solid solutions, alloys of immiscible elements, several kinds of compounds and composites [6–9].

Although the precise mechanism of the mechanical alloying process is thought to involve the repeated fracture and welding of powder particles during ball-powder-ball and ball-powder-container collisions, alloying takes place then by the atomic interdiffusion across welded interfaces of grain powders.

The aim of the present work is first to produce the binary Fe<sub>50</sub>Ni<sub>50</sub> system by high-energy ball alloying technique. Several alloying times ranged from 1 and 322 h are considered. The powders were investigated by means of microstructural observations by scanning microscopy, X-ray diffraction and <sup>57</sup>Fe Mössbauer spectrometry.

\* Corresponding author.

E-mail address: [abdel\\_djekoun@yahoo.fr](mailto:abdel_djekoun@yahoo.fr) (A. Djekoun).

## 2. Experimental techniques

Mechanical alloying as mixture of pure Fe (99.9%) powder and Ni (99.8%) powder was carried out in a commercial Fritsch Pulverisette 7 planetary ball mill. To prevent oxidation phenomena, the mixed powder was sealed in a cylindrical vial under an argon atmosphere with stainless steel balls. The weight ratio of balls to powder was 20:1. The milling intensity  $I = 8$  corresponding to vial rotation speed of  $\sim 1124$  tr/min was used. To avoid excessive heating during milling, each 30 min of milling was followed by a stay during 10 min under the argon atmosphere at room temperature. After different milling times, the process was interrupted and small amounts of milled powders were taken out for analysis.

X-ray diffraction patterns were recorded using D501 SIEMENS diffractometer (with monochromatised Cu  $K\alpha$  radiation;  $\lambda_{\alpha} = 1.542056$  Å), in the  $2\theta$  range from  $30^\circ$  to  $140^\circ$ . X-ray patterns were analysed by MAUD program [10], which is based on the Rietveld method [11] combined with a Fourier analysis. This procedure is well adapted for diffraction patterns which exhibit broadened diffraction peaks. This method thus allows the refinement of the structural and microstructural parameters, the lattice parameters and the size and the microstrains of crystalline domains. Scanning electron microscopy has been used for morphology and microstructure observations. Mössbauer spectra were taken at 300 K in a transmission geometry with conventional constant acceleration spectrometer, using a radioactive  $^{57}\text{Co}$  source diffused into a rhodium matrix. Velocity was controlled using a natural  $\alpha$ -Fe foil and isomer shift values are quoted to that of  $\alpha$ -Fe spectrum at room temperature and the spectra were fitted using the MOSFIT program [12].

## 3. Results and discussion

### 3.1. X-ray diffraction studies

Fig. 1 shows the evolution of X-ray diffraction (XRD) Cu  $K\alpha$  patterns as a function of milling time for the  $\text{Fe}_{50}\text{Ni}_{50}$

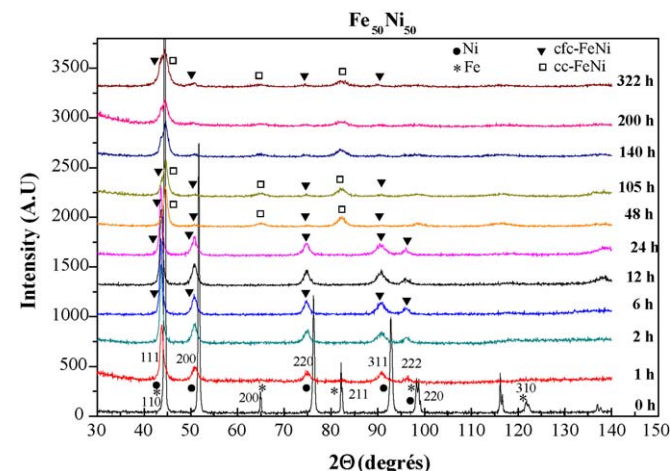


Fig. 1. X-ray diffraction patterns of  $\text{Fe}_{50}\text{Ni}_{50}$  powdered alloys synthesised in high-energy mill for various milling times.

powders. One clearly observes that (i) the diffraction Bragg peaks broaden, with increasing milling times and (ii) the occurrence of one or two structural type phases. This suggests a continuous decrease of the grain size and the atomic interdiffusion process is a priori dependent on the alloying time. XRD (marked 0 h milled) shows reflections corresponding to bcc Fe and fcc Ni metals. After 1 h of milling the reflection peaks (2 0 0), (2 1 1) corresponding to the bcc  $\alpha$ -Fe disappear and only the reflections corresponding to fcc phase are present with the peaks slightly shifted towards lower angles. A little angular shift, attributed to incipient formation of  $\text{Fe}_{50}\text{Ni}_{50}$  alloy and to the first order internal stresses induced by milling. The first order internal stresses act at the macroscopic level by modifying the lattice parameter and consequently produce an angular shift of the XRD peak [13]. This shift is very well defined for 2 h of milling and increases continuously with milling time. The characteristic Ni lines gradually decrease in amplitude and decay after 48 h milling. This effect proves that Ni atoms dissolve in the iron lattice entirely. We observed a formation of mixture of phases as fcc  $\text{FeNi}$  solid solution  $\gamma$  (Fe, Ni) (called taenite) space group  $Fm\bar{3}m$  and bcc (Fe, Ni). The (2 0 0) reflection which is weak in intensity appears to have disappeared for higher milling times due to line broadening and merging with the background. The high angle diffraction lines become broader and broader until their complete disappearance. The increase in line broadening with milling time is due to both the reduction in grain size and increase in lattice strain [14] on milling. The estimation of the lattice parameter, the crystallite size and the microstrains was obtained from refinement of X-ray patterns using Maud procedure. Fig. 2 shows the variation of Fe–Ni crystallite average size versus milling time. As can be seen in Fig. 2, during the early stage of milling the crystallite size decreases rapidly in the beginning of milling and slows down afterwards and becomes gradually smaller with increasing milling time with a final value of about 5 nm. This value is smaller than the 45 nm [15] and 16.5 nm [16] for the iron–nickel ultra-fine particles obtained by a gas-condensation method, with the same composition. The lattice parameters (a) for  $\gamma$  (Fe, Ni) are plotted in Fig. 3 as a function of milling time. The value of lattice parameters increased from  $a = 0.3587$  nm for 1 h to 0.3601 nm for 322 h of milling. It is

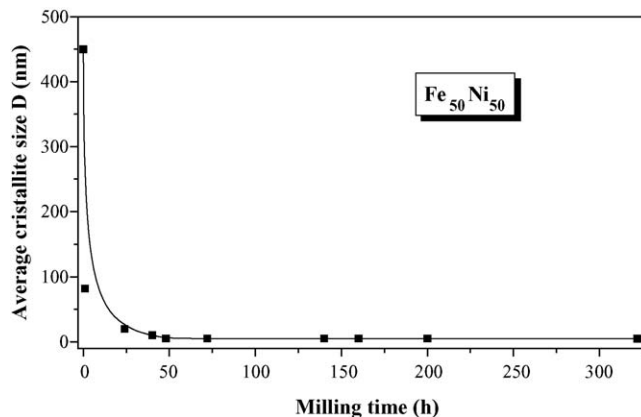


Fig. 2. Crystallite size of the Fe–Ni powders as function of milling time.

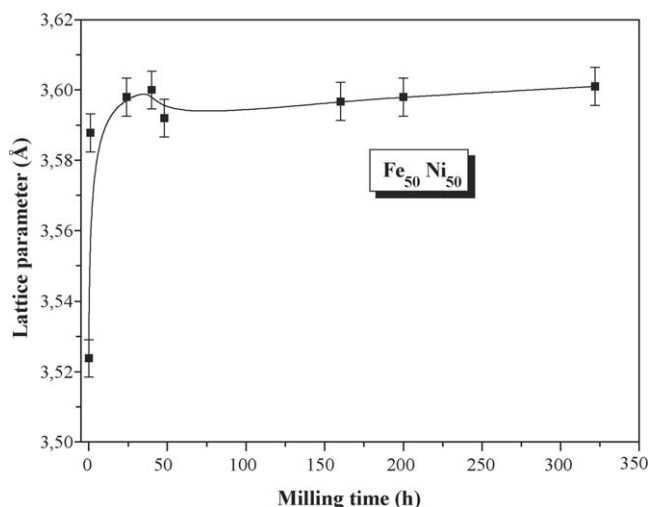


Fig. 3. Lattice parameter of  $\gamma$  (Fe, Ni) powders synthesised in high-energy mill for various milling times.

slightly higher than the value of 0.35975 nm reported for the bulk FeNi alloy. Such a minute evolution in the lattice parameter is conceivable since the atomic radii of Fe and Ni are close [17]. The increase in lattice parameter with milling time is due to the disordering of the alloy as observed by Olezak et al. [18] in the case Fe–Al. The lattice microstrains obtained as a consequence of the alloying process increase with milling time and reach the final value of 0.021% as seen in Fig. 4.

### 3.2. Microstructure

The morphologies of Fe–Ni powders after various milling times are shown in Figs. 5 and 6. It can be seen that different morphologies are present during the mechanical alloying stages. As a result of intensive fracture and cold welding as shown in Fig. 5(a and b, respectively), composite particles are formed for short milling time. With increasing milling time, the particles change into a flake or platelet shape (Fig. 6a). Some with a layered structure, constituted of alternate Ni and Fe layers is observed (Fig. 6b), typical of materials prepared by mechanical alloying for ductile or brittle elements [19,20]. The layered structure may be caused by heavy plastic deformation, because

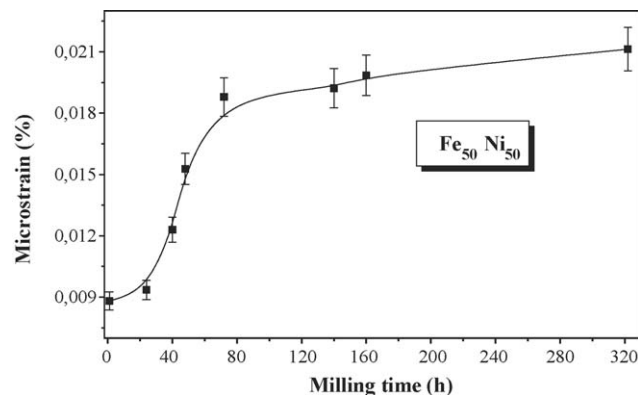


Fig. 4. Lattice microstrains of  $\gamma$  (Fe, Ni) powders synthesised in high-energy mill for various milling times.

the balls impact repeatedly with high energy. These layers are gradually destroyed under repeated shock effect of balls on the powder. The lamellar structure is progressively refined and convoluted by repeated flattening, fracturing and welding actions [21]. With milling time up to 33 h, the large amount of flakes is reduced and the flake particles become ground in to round particles (Fig. 6c). By increased milling times, the mechanical alloying progress and the refinement of the structure continues. Finally, for a long milling time, powder particles are equiaxed and relatively homogenous in size (Fig. 6d and e).

### 3.3. Mössbauer studies

The Mössbauer measurements were applied in order to monitor the alloy evolution at every stage of the milling process. The room temperature Mössbauer spectra taken at different times are shown in Fig. 7a. For the unmixed sample, the spectrum shows the presence of a typical sextet characterized by a hyperfine field of  $H = 33.0$  T corresponding to the  $\alpha$ -Fe present in the unmixed mixture of the Fe–Ni powder. Between 2 and 33 h of milling, the Mössbauer spectrum showed a presence of a magnetic sextet and a distribution of hyperfine fields with a probable hyperfine value  $H_p = 31.2$  T (Fig. 7b), with asymmetric intensities with very broadened lines, typical for Fe–Ni disorder alloys in the

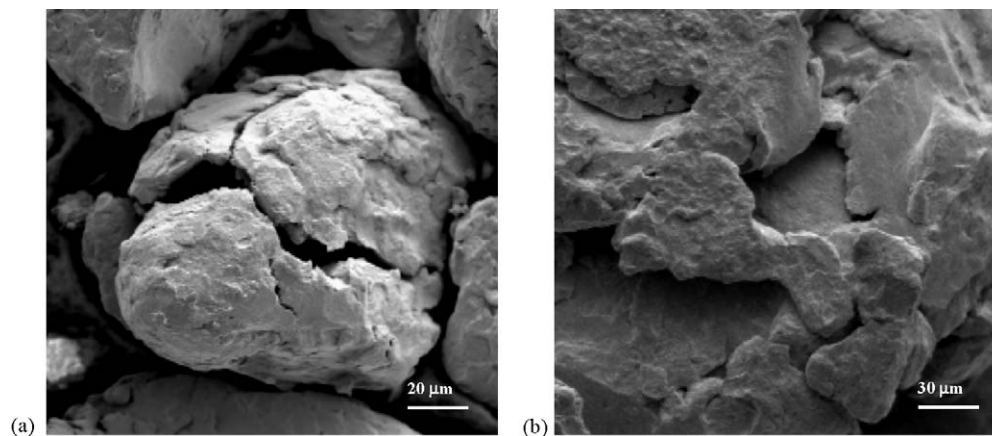


Fig. 5. SEM micrograph of (Fe, Ni) powders shows fracture (a) and cold welding (b) in mechanical alloying.



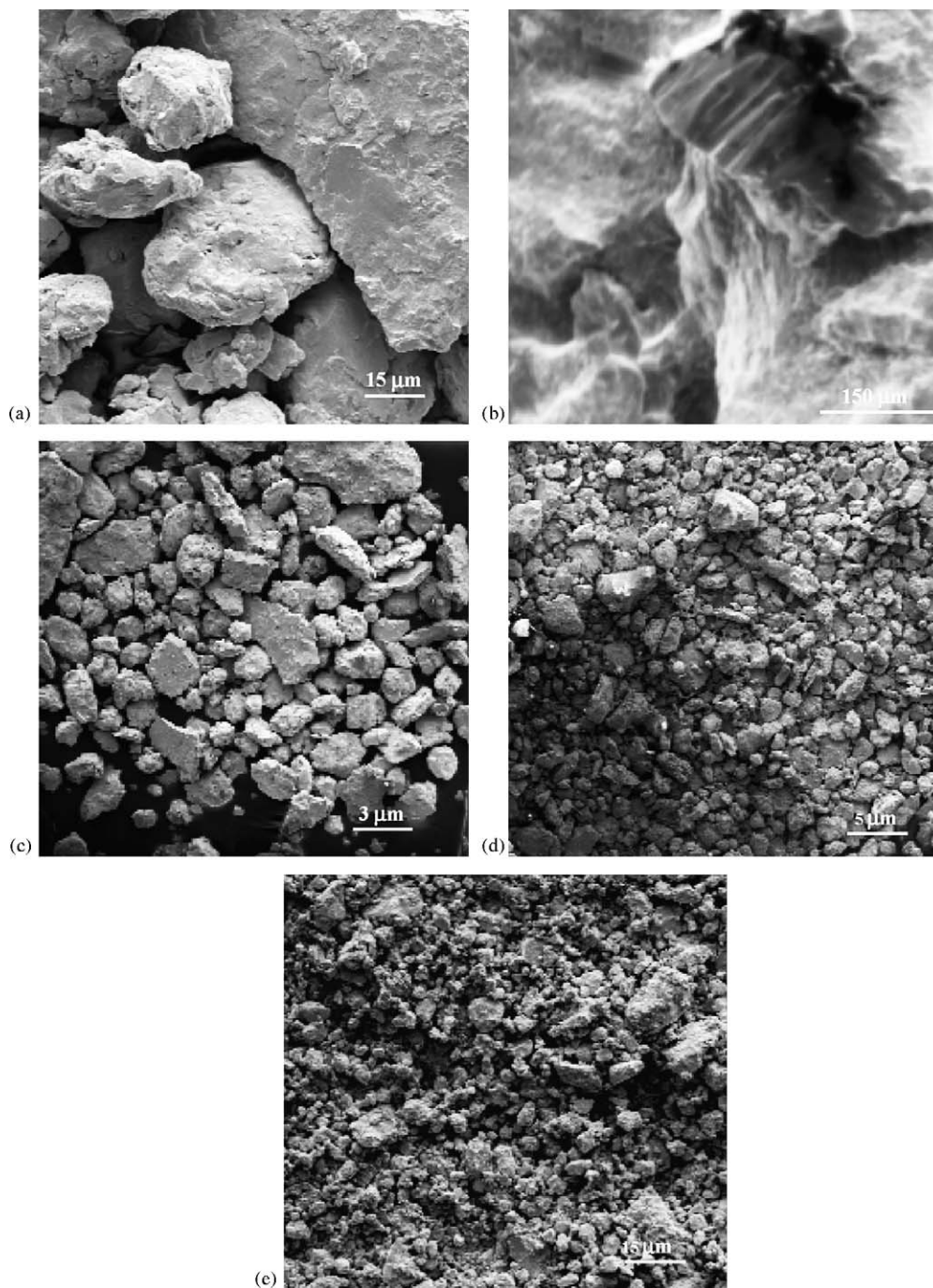


Fig. 6. SEM Micrograph of (Fe, Ni) powders prepared by mechanical alloying after different milling times (a) 3 h; (b) lamellar structure; (c) 33 h; (d) 72 h; (e) 200 h.

composition range 35–50% Ni, can be attributed to Fe–Ni  $\gamma$  phase (Ni-rich taenite). This broadening arises due to the alloying progress, the grain size reduction and the increasing microstrains. After the mixing time 48 h, the Mössbauer spectrum at room temperature (Fig. 7a) exhibits clearly the coexistence of Fe–Ni phases with different composition, a magnetic phase corresponding to a  $\alpha$  (bcc) FeNi phase and a paramagnetic phase attributed to a  $\gamma$  (fcc) FeNi phase with a concentration of about  $\sim 30$  at.% Ni. This agrees with results obtained for the formation of FeNi phase by a gas condensation method [16] and by chemical reduction [22] with the same

composition. On the other hand, Ping, Rancourt and Dunlap [23] worked recently with splat-quenched Fe–Ni alloys in the composition range of 5–70 at.% Fe. Mössbauer spectra at RT were used to confirm that for 30 at.% Ni (70 at.% Fe) the spectrum consists of a single line well defined ascribed to dynamic effects. We also note that the paramagnetic phase increases as function of milling time to the detriment of the magnetic phase (Fig. 8). This paramagnetic component is due to the presence of superparamagnetic particles [24–26]. The fitting of the spectra resulted in the hyperfine magnetic fields distributions,  $P(B_{\text{hf}})$ , shown in Fig. 7b. They are relatively

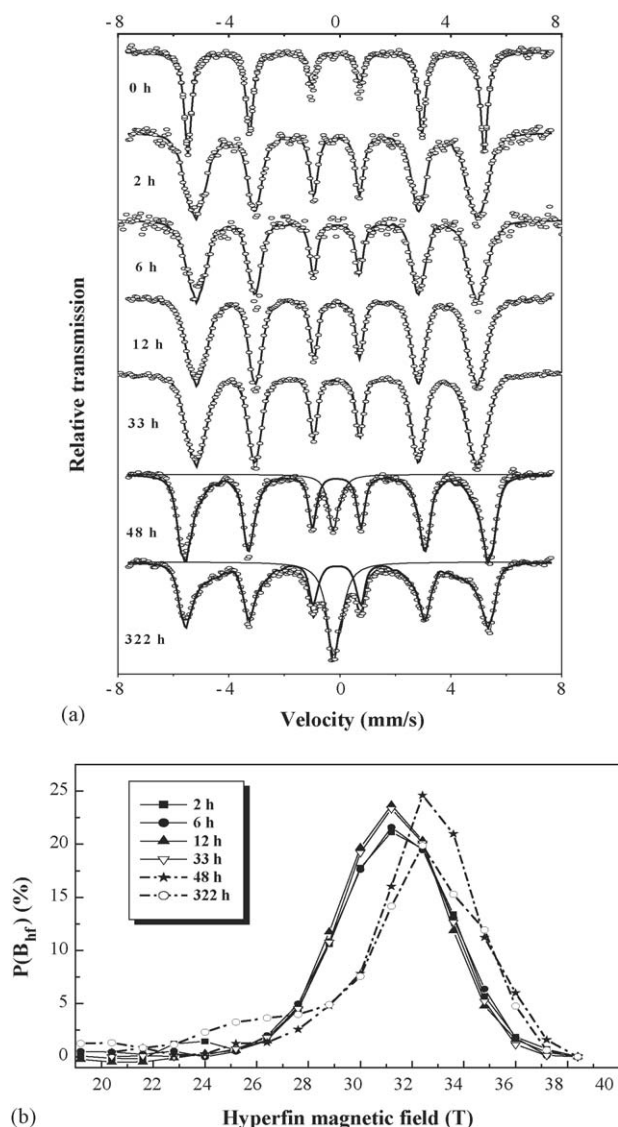


Fig. 7. Mössbauer spectra (a) and hyperfine field distributions (b) at room temperature for  $\text{Fe}_{50}\text{Ni}_{50}$  powders after different milling times.

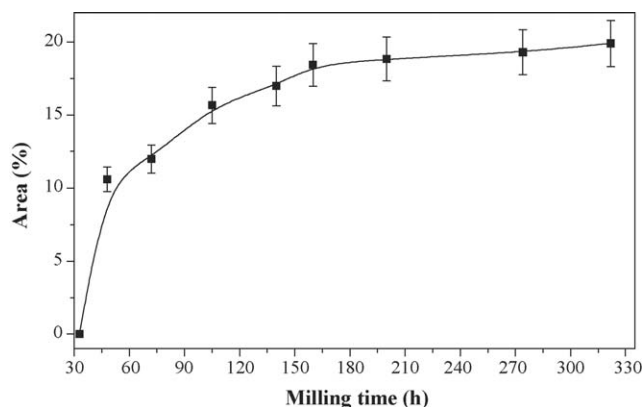


Fig. 8. Evolution of the paramagnetic phase of the  $\text{Fe}_{50}\text{Ni}_{50}$  powders as function of milling time.

broad because of the high lattice strains, defects and high density of the grain boundaries in the milled alloy. We observe that the maximum of the distribution  $H_i = 32.4$  T is slightly shifted to the larger magnetic field for the 48–322 h milled alloy.

#### 4. Conclusion

Fe–Ni alloy was prepared by mechanical alloying technique in a high-energy planetary ball mill. The examination by SEM reveals that in the early stage of milling a multilayer is formed. Longer processing time leads to the formation of uniform and homogeneous structure. The as-milled samples, characterized by X-ray diffraction, contain a mixture of  $\alpha$  (bcc) and  $\gamma$  (fcc) phases with a nanoscale grain size (determined by Maud program). The lattice parameter expands on disordering by ball milling. A paramagnetic phase appears after 48 h of ball milling detected by Mössbauer spectroscopy is attributed to a  $\gamma$  (fcc) FeNi phase with a concentration of about  $\approx 30$  at.% Ni.

#### Acknowledgement

Anne-Marie Mercier (Université du Maine) is gratefully acknowledged for her help in performing X-ray diffraction experiments.

#### References

- [1] H. Gleiter, P. Marquardt, Z. Metall. 75 (1984) 263.
- [2] H. Fecht, E. Hellstern, Z. Fu, W.L. Johnson, Met. Trans. A 21 (1990) 2333.
- [3] J. Eckert, C.E. Krill III, W.L. Johnson, J. Mater. Res. 7 (1992) 1751.
- [4] M.A. Morris, D.G. Morris, J. Mater. Sci. 26 (1991) 4687.
- [5] H. Gleiter, J. Appl. Cryst. 24 (1991) 79.
- [6] M. Trudeau, R. Schultz, Mater. Sci. Eng. A 134 (1991) 1361.
- [7] T.D. Shen, K.Y. Wong, H.X. Quan, J.T. Wang, J. Appl. Phys. 71 (1992) 1967.
- [8] P. Schaaf, G. Rixecker, E. Yang, C.N.J. Wagner, U. Gonser, Hyperfine Interact. 94 (1994) 2239.
- [9] A.R. Yavari, P.J. Desre, T. Benamer, Phys. Rev. Lett. 68 (1992) 2235.
- [10] L. Lutterotti, MAUD CPD, Newsletter (IUCr) 24 (2000).
- [11] H.M. Rietveld, J. Appl. Crystallogr. 2 (1996) 65.
- [12] J. Teillet, F. Varret, Mosfit Programm, University du Maine, unpublished.
- [13] L. Castex, J.L. Lebrun, G. Maeder, J.M. Sprauel, Détermination de contraintes résiduelles par diffraction des rayons X, vol. 22, Publications scientifiques et techniques de l'ENSAM, Paris, 1981, p. 51.
- [14] C. Kuhrt, L. Shultz, J. Appl. Phys. 73 (1993) 1221.
- [15] A. Djekoun, B. Bouzabata, S. Alleg, J.M. Grenèche, A. Otmani, Ann. Chim. Sci. Mater. 23 (1998) 557.
- [16] R.B. Scorzelli, E. Galvao da Silva, C. Kaito, Y. Saito, M. McElfresh, M. Elmassalami, Hyperfine Interact. 94 (1994) 2337.
- [17] C. Kittel, Introduction to Solid State Physics, Wiley, New York, 1966.
- [18] D. Olezak, Mater. Sci. Eng. A181/182 (1994) 121.
- [19] R.M. Davis, B. Mc Dermot, C.C. Koch, Met. Trans. 19A (1988) 28.
- [20] A. Otmani, B. Bouzabata, A. Djekoun, S. Alleg, Ann. Chim. Sci. Mater. 22 (1997) 201.
- [21] J.S. Benjamin, Metall. Trans. 1 (1970) 2943.
- [22] E. Lima Jr., V. Drago, R. Bolsoni, P.F.P. Fichtener, Solid State Commun. 125 (2003) 265.
- [23] J.Y. Ping, D.G. Rancourt, R.A. Dunlap, J. Magn. Magn. Mater. 103 (1992) 285.
- [24] A.P. Fulde, R.E. Watson, Phys. Rev. B 8 (1973) 440.
- [25] H.N. Ok, M.S. Han, J. Appl. Phys. 44 (1973) 1932.
- [26] R.H. Lindquist, G. Constabaris, W. Kündig, A.M. Portis, J. Appl. Phys. 39 (1968) 1001.